

Simplified Space Vector Based Hybrid PWM Algorithm for Reduced Current Ripple

N. Ravisankar Reddy¹, T. Brahmananda Reddy¹, J. Amarnath², and D. Subba Rayudu¹

¹E.E.E Department, G. Pulla Reddy Engineering College, Andhra Pradesh, India

Email: netapallyravi@gmail.com

²E.E.E Department, J.N.T. University, Hyderabad, Andhra Pradesh, India

Email: {amarnathjinka, tbnr}@rediffmail.com

Abstract—This paper presents a simplified hybrid pulsewidth modulation (HPWM) algorithm to reduce the steady state ripple in current. In the conventional space vector PWM (CSVPWM) algorithm, the zero voltage applying time is distributed equally in every sampling interval. Also, this paper deals with two discontinuous PWM (DPWM) algorithms, which use only one zero state in each sampling interval. The proposed PWM algorithm is designed based on the notion of stator flux ripple. Modulation index and duty cycle dependent expression for rms value of the stator flux over a sampling interval is calculated. The rms flux ripple characteristics are graphically illustrated, from which the proposed hybrid PWM algorithm is developed. The proposed algorithm results in simultaneous reduction of harmonic distortion at all modulation indices. To validate the above proposed method, simulation studies have been carried out on v/f induction motor drive and the results have been presented and analyzed.

Index Terms— conventional SVPWM, discontinuous PWM, stator flux ripple

I. INTRODUCTION

Improvements in fast switching power devices have led to an increased interest in voltage source inverters (VSI) with pulsewidth modulation (PWM) control. PWM-VSI fed induction motor drives have continuously drawn the attention of many researchers all around the world. Several PWM algorithms exist, and a survey of these was given in [1]. Out of several approaches, triangular comparison (TC) approach and space vector (SV) approach are main implementation techniques [2]. Conventional space vector PWM (CSVPWM) [3] is popular and widely used PWM strategy, which has the advantages of lower current harmonics and a possible higher modulation index compared with the sine-triangle PWM method.

In the CSVPWM, the reference voltage vector situated in the appropriate sector is approximated by the time averaging over a subcycle of the two adjacent active states and the two zero states [2]. The CSVPWM algorithm employs equal division of zero voltage vector times within a sampling interval. However, by utilizing the freedom of zero state division, various DPWM methods can be generated. The DPWM methods give less harmonic distortion at higher modulation indices compared to CSVPWM and less switching losses at all modulation indices. Few hybrid PWM algorithms have

been developed for reduced current ripple at all modulation indices in [4-7]. In these algorithms, expressions for rms stator flux ripple for each sequence are derived. Whereas [8] uses a single expression using the conventional space vector approach, which increases the complexity of the algorithm.

This paper presents simplified hybrid PWM algorithm for reduced current ripple. The proposed algorithm uses the concept of imaginary switching times for reduced complexity. The proposed hybrid PWM algorithm employs the switching sequence, which results in the lowest harmonic distortion in the current over the given sampling interval.

II. PROPOSED SWITCHING SEQUENCES

A 3-phase, two-level VSI has eight possible switching states, can be depicted as voltage space vectors as shown in Fig. 1. The space vector locations form the vertices of a regular hexagon, forming six symmetrical sectors.

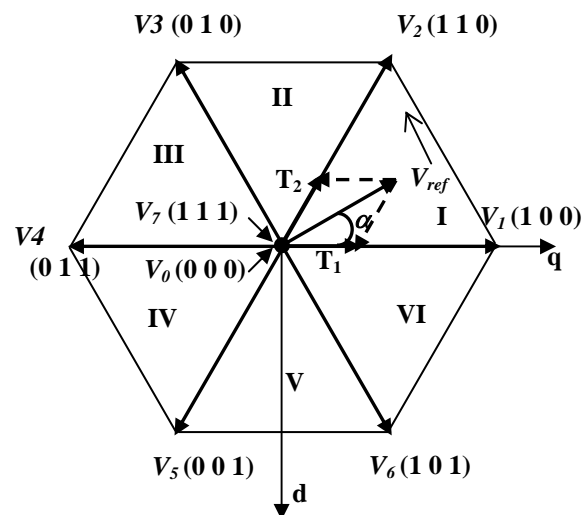


Fig. 1 Voltage space vectors produced by an inverter

In the CSVPWM, the reference voltage vector situated in the appropriate sector is approximated by the time averaging over a sampling interval of the two adjacent active voltage vectors and two zero voltage vectors. The switching turn-on times of the two active states and two zero states are utilized to determine the duty cycle information to program the active switching gate signals. When the inverter is operating in the linear modulation region, the sum of the times the two active states are

utilized is less than the duration of the subcycle, in which case the remaining time is occupied by using the two zero states. The expressions for the active states time durations and zero states time duration in first sector can be given as:

$$T_1 = \frac{2\sqrt{3}}{\pi} M_i (\sin(60^\circ - \alpha)) T_s \quad (1)$$

$$T_2 = \frac{2\sqrt{3}}{\pi} M_i (\sin \alpha) T_s \quad (2)$$

$$T_Z = T_s - T_1 - T_2 \quad (3)$$

In the proposed algorithm, the switching times can be calculated by using the concept of imaginary switching times which uses instantaneous values of the reference voltages of a, b and c phases. This method does not depend on the magnitude of the reference voltage space vector and its relative angle with respect to the reference axis. The imaginary switching time periods proportional to the instantaneous values of the reference phase voltages are defined as [7, 9-10]

$$T_{an} \equiv \left(\frac{T_s}{V_{dc}} \right) V_{an}$$

$$T_{bn} \equiv \left(\frac{T_s}{V_{dc}} \right) V_{bn} \quad (4)$$

$$T_{cn} \equiv \left(\frac{T_s}{V_{dc}} \right) V_{cn}$$

Here V_{an} , V_{bn} and V_{cn} are the instantaneous voltages. The switching times T_{an} , T_{bn} and T_{cn} could be negative when the instantaneous reference voltages are negative. Hence, these times are called as imaginary switching times. The active vector switching times can be calculated in each sampling interval as follows:

Let

$$T_{Max} = \text{Max}(T_{an}, T_{bn}, T_{cn}) \quad (5)$$

$$T_{Min} = \text{Min}(T_{an}, T_{bn}, T_{cn}) \quad (6)$$

$$T_{Mid} = \text{Mid}(T_{an}, T_{bn}, T_{cn}) \quad (7)$$

where Max, Min and Mid are the nominal values used during the sampling interval. The function $\text{Max}(T_{an}, T_{bn}, T_{cn})$ selects the maximum value among T_{an} , T_{bn} and T_{cn} . Similarly $\text{Min}(T_{an}, T_{bn}, T_{cn})$ selects the minimum value and $\text{Mid}(T_{an}, T_{bn}, T_{cn})$ selects the middle value. Finally, the active state times T_1 and T_2 may be expressed as

$$T_1 = T_{Max} - T_{Mid} \text{ and } T_2 = T_{Mid} - T_{Min} \quad (8)$$

The zero voltage vector time can be calculated by using (3). The conventional SVPWM algorithm employs equal division of zero voltage vector times within a sampling interval. However, by utilizing the freedom of zero state division, various DPWM methods can be generated. In the proposed method the zero state time will be shared between two zero states as T_0 for V_0 and T_7 for V_7 respectively, and can be expressed as [6]

$$T_0 = k_o T_z \quad (9)$$

$$T_7 = (1 - k_o) T_z \quad (10)$$

If $k_o = 0.5$, then the CSVPWM algorithm is obtained. When $k_o = 0$, any one of the phases is clamped to positive dc bus for 120 degrees over a fundamental interval and then DPWMMAX is obtained. When $k_o = 1$, any one of the phases is clamped to negative dc bus for 120 degrees over a fundamental interval and then DPWMMIN is obtained. Thus, in the first sector, CSVPWM uses 0127-7210 sequence, DPWMMAX uses 721-127 sequence and DPWMMIN uses 012-210 sequence. Various DPWM algorithms can be generated with step change of k_o between zero and one. Moreover, by shifting the third harmonic signal from 0° to 120° infinite number of DPWM methods can be generated. Here, $k_o = 1$ when the third harmonic signal is negative and $k_o = 0$ when the third harmonic signal is positive. In the DPWM methods, any one of the phases is clamped to the positive or negative dc bus for at most a total of 120° over a fundamental cycle. Hence, the switching losses of the associated inverter leg are eliminated. Moreover, within a sampling interval three switchings will occur in CSVPWM algorithm whereas two switchings in DPWM algorithms. Hence, the switching frequency of DPWM algorithms is reduced by 33% compares with CSVPWM. Hence a switching frequency coefficient is introduced as defined in (11).

$$k_{sw} = \frac{f_{swCSVPWM}}{f_{swDPWM}} \quad (11)$$

III. ANALYSIS OF FLUX RIPPLE IN A SAMPLING INTERVAL

In the space vector approach, the applied voltage vector equals the reference voltage vector only in an average sense over the given sampling interval, and not in an instantaneous fashion. The difference between applied voltage vector and reference voltage vector is the ripple voltage vector, which depends on space and modulation index. The ripple voltage vectors and trajectory of the stator flux ripple can be represented in a complex plane as shown in Fig 2. The corresponding d-axis and q-axis components of the stator flux ripple vector are as shown in Fig 3, from which it can be observed that the application of a zero voltage vector results in a variation of the q-axis component of the flux ripple and the application of any active voltage vector results in variation of the both the d-axis and q-axis components.

The error volt-seconds corresponding to the voltage ripple vectors are given by

$$V_{r1} T_1 = \left(\frac{2}{3} V_{dc} \sin \alpha \right) T_1 + j \left(\frac{2}{3} V_{dc} \cos \alpha - V_{ref} \right) T_1 \quad (12)$$

$$V_{r2} T_2 = - \left(\frac{2}{3} V_{dc} \sin(60^\circ - \alpha) \right) T_2 + j \left(\frac{2}{3} V_{dc} \cos(60^\circ - \alpha) - V_{ref} \right) T_2 \quad (13)$$

$$V_{r0} T_0 = -j V_{ref} T_0 = -j \frac{2M_i V_{dc}}{\pi} T_0 = j \lambda_{q0} \quad (14)$$

$$V_{r7}T_7 = -jV_{ref}T_7 = -j\frac{2M_iV_{dc}}{\pi}T_7 = j\lambda_{q7} \quad (15)$$

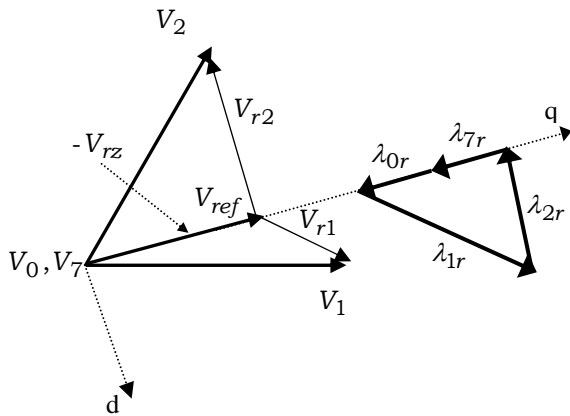


Fig. 2 voltage ripple vectors and trajectory of the stator flux ripple

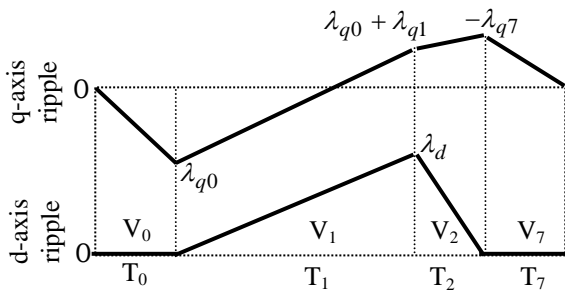


Fig. 3 q-axis and d-axis components of the stator flux ripple vectors From (1) and (2)

$$\sin \alpha = \frac{\pi T_2}{2\sqrt{3}M_i T_s} \quad (16)$$

$$\cos \alpha = \frac{\pi(T_1 + 0.5T_2)}{3M_i T_s} \quad (17)$$

$$\cos(60^\circ - \alpha) = \frac{\pi(0.5T_1 + T_2)}{3M_i T_s} \quad (18)$$

$$\text{and } \left(\frac{2}{3}V_{dc} \sin \alpha\right)T_1 = \left(\frac{2}{3}V_{dc} \sin(60^\circ - \alpha)\right)T_2 \quad (19)$$

By substituting (16) - (19) in (12) and (13),

$$V_{r1}T_1 = \frac{\pi V_{dc}}{3\sqrt{3}M_i} \frac{T_1 T_2}{T_s} + j\left(\frac{2V_{dc}\pi(T_1 + 0.5T_2)}{9M_i T_s} - \frac{2V_{dc}M_i}{\pi}\right)T_1 = \lambda_d + j\lambda_{q1} \quad (20)$$

$$V_{r2}T_2 = -\frac{\pi V_{dc}}{3\sqrt{3}M_i} \frac{T_1 T_2}{T_s} + j\left(\frac{2V_{dc}\pi(0.5T_1 + T_2)}{9M_i T_s} - \frac{2V_{dc}M_i}{\pi}\right)T_2 = -\lambda_d + j\lambda_{q2} \quad (21)$$

The q-axis ripple and d-axis ripple are given in (22) and (23).

$$\begin{aligned} \lambda_q &= \frac{\lambda_{q0}t}{T_0}, \quad \text{if } 0 \leq t \leq T_0 \\ &= \lambda_{q0} + \frac{\lambda_{q1}}{T_1}t_1, \quad \text{if } T_0 \leq t \leq (T_0 + T_1) \\ &= \lambda_{q0} + \lambda_{q1} + \frac{\lambda_{q2}}{T_2}t_2, \quad \text{if } (T_0 + T_1) \leq t \leq (T_0 + T_1 + T_2) \\ &= -\lambda_{q7} + \frac{\lambda_{q7}}{T_7}t_3, \quad \text{if } (T_s - T_7) \leq t \leq T_s \end{aligned} \quad (22)$$

$$\begin{aligned} \lambda_d &= 0, \quad \text{if } 0 \leq t \leq T_0 \\ &= \frac{\lambda_d}{T_1}t_1, \quad \text{if } T_0 \leq t \leq (T_0 + T_1) \\ &= \lambda_d - \frac{\lambda_d}{T_2}t_2, \quad \text{if } (T_0 + T_1) \leq t \leq (T_0 + T_1 + T_2) \\ &= 0, \quad \text{if } (T_s - T_7) \leq t \leq T_s \end{aligned} \quad (23)$$

where,

$$t_1 = t - T_0; \quad t_2 = t - T_0 - T_1; \quad t_3 = t - T_0 - T_1 - T_2 \quad (24)$$

The mean square stator flux ripple over a sampling interval can be calculated as

$$\begin{aligned} \lambda^2_{(rms)} &= \frac{1}{T_s} \int_0^{T_s} \lambda_q^2 dt + \frac{1}{T_s} \int_0^{T_s} \lambda_d^2 dt \\ &= \frac{1}{3} \left\{ \lambda_{q0}^2 \frac{T_0}{T_s} + \left[\lambda_{q0}^2 + (\lambda_{q0} + \lambda_{q1})^2 + \lambda_{q0}(\lambda_{q0} + \lambda_{q1}) \right] \frac{T_1}{T_s} + \left[(\lambda_{q0} + \lambda_{q1})^2 - \lambda_{q7}(\lambda_{q0} + \lambda_{q1}) + \lambda_{q7}^2 \right] \frac{T_2}{T_s} + \lambda_{q7}^2 \frac{T_7}{T_s} + \lambda_d^2 \frac{(T_1 + T_2)}{T_s} \right\} \end{aligned} \quad (25)$$

By using the above formula, the mean square flux ripple can be easily computed and graphically represented for various PWM methods.

IV. PROPOSED HYBRID PWM ALGORITHM

The mean square flux ripple characteristics obtained from (25) for various PWM algorithms are compared for different modulation indices and given in Fig.4 – Fig.6.

From the figures it can be observed that, the conventional SVPWM algorithm gives higher harmonic distortion at higher modulation indices when compared to DPWM algorithms. Hence, to reduce the current ripple at all modulation indices, the hybrid PWM (HPWM) algorithm is proposed in this paper.

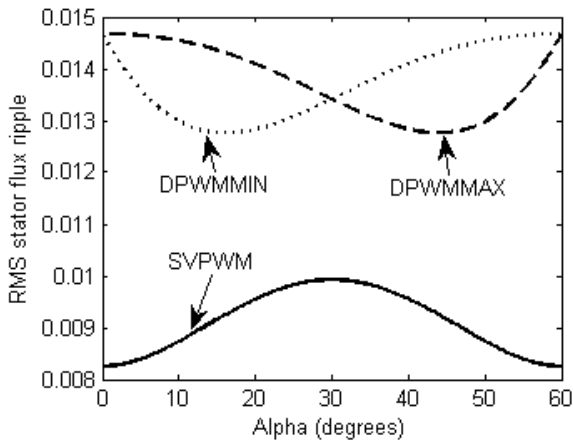


Fig. 4 Variation of stator flux ripple over the first sector for $M_i = 0.4$

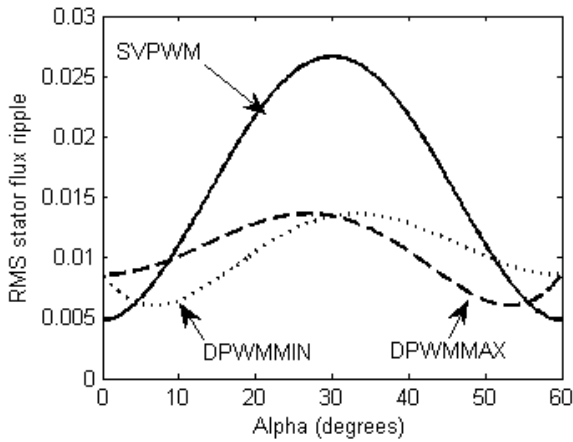


Fig. 5 Variation of stator flux ripple over the first sector for $M_i = 0.8$

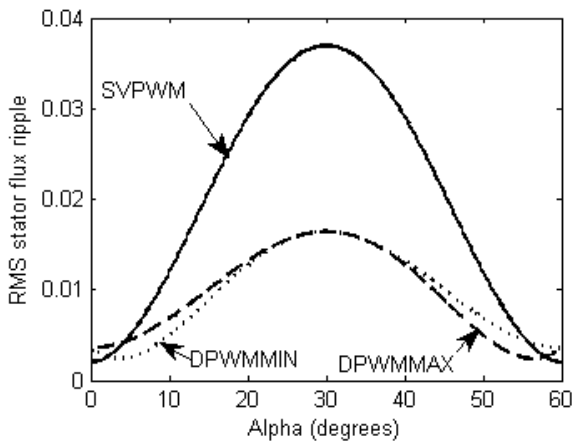


Fig. 6 Variation of stator flux ripple over the first sector for $M_i = 0.906$

The proposed HPWM algorithm consists of a set of PWM algorithms and employs the best algorithm, which gives less ripple for given modulation index.

V. SIMULATION RESULTS AND DISCUSSION

The proposed PWM algorithm is tested on v/f controlled induction motor drive. The motor parameters are as follows:

Stator resistance $R_s = 1.57$ ohm, rotor resistance $R_r = 1.21$ ohm, stator inductance $L_s=0.17$ H, rotor inductance $L_r=0.17$ H, mutual inductance $L_m=0.165$ H, moment of inertia $J=0.089$ Kg-m².

Simulation studies are carried out at various modulation indices. Fig. 7 – Fig. 12 show the steady state current waveforms along with harmonic distortion. From the simulation results, it can be observed that the proposed PWM algorithm gives less harmonic distortion in comparison with conventional SVPWM algorithm.

VI. CONCLUSIONS

The conventional SVPWM algorithm needs angle and sector information to calculate switching times, which increases the complexity of the algorithm. Moreover, SVPWM algorithm gives inferior performance over DPWM algorithm at higher modulation indices and at the same time DPWM methods give inferior performance at lower modulation indices. Hence, to overcome these problems, this paper presents HPWM algorithm, which combines both SVPWM algorithm and DPWM algorithms and gives superior performance at all modulation indices. Also, to reduce the complexity involved, the proposed algorithm uses the concept of imaginary switching times.

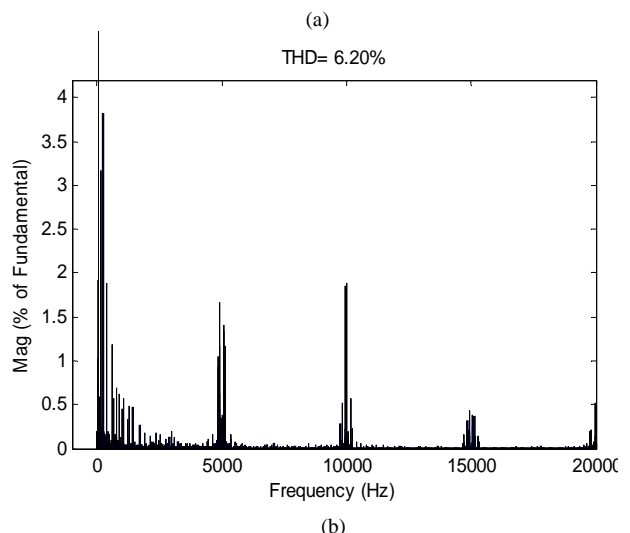
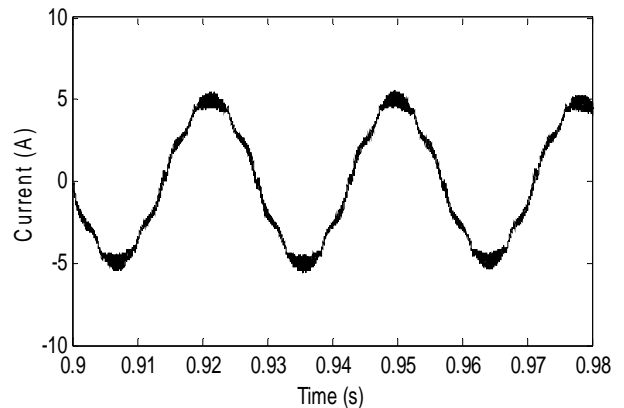
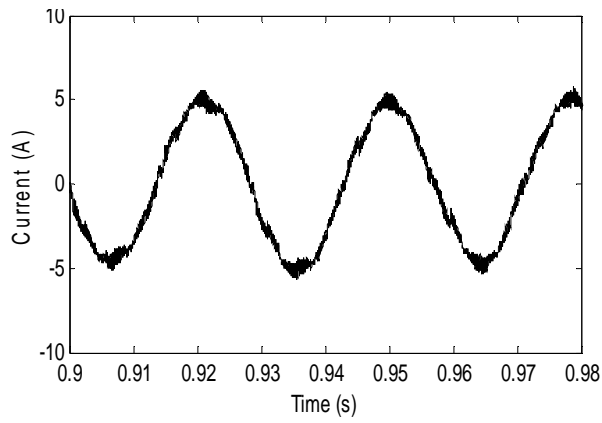
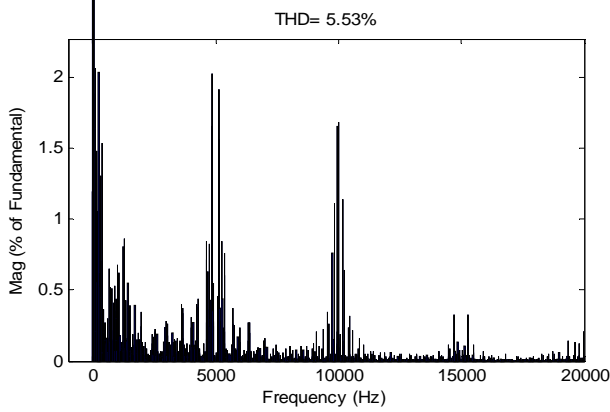


Fig. 7 Steady state current along with THD with SVPWM algorithm for $M_i = 0.72$

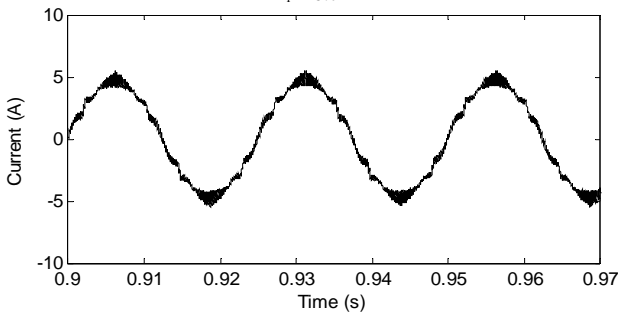


(a)

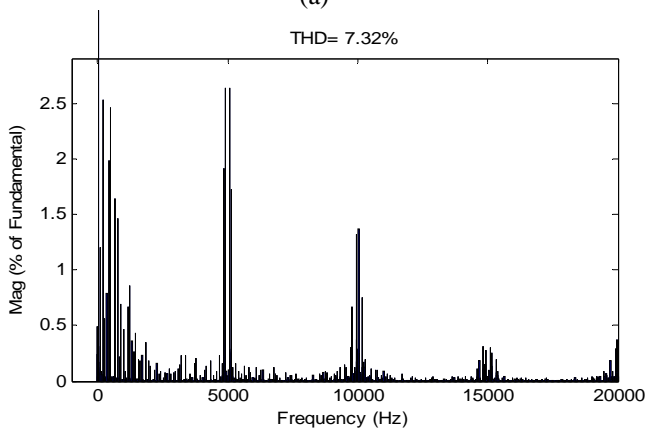


(b)

Fig. 8 Steady state current along with THD with HPWM algorithm for $M_i = 0.72$

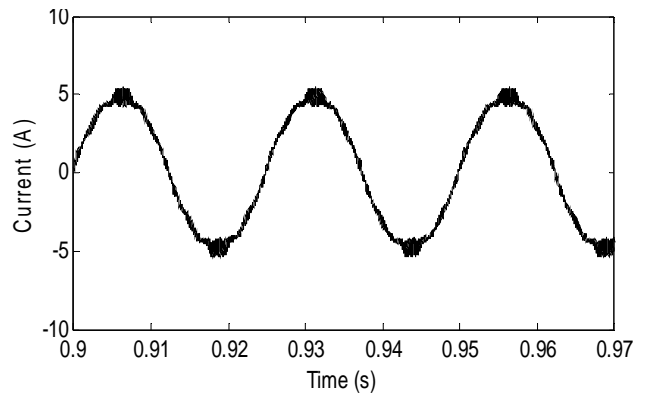


(a)

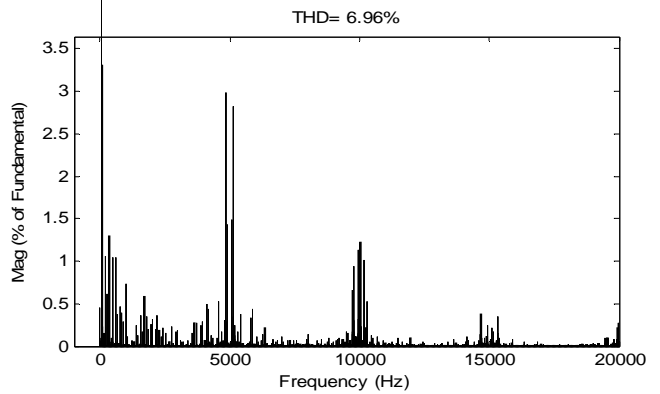


(b)

Fig. 9 Steady state current along with THD with SVPWM algorithm for $M_i = 0.81$

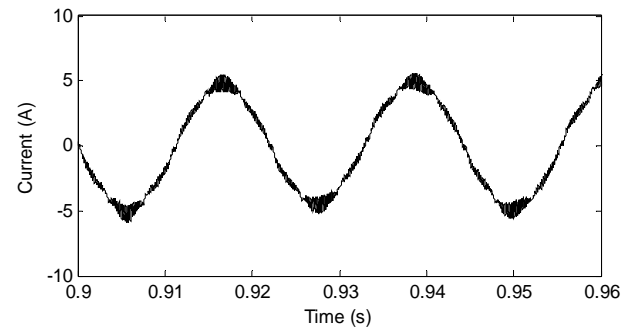


(a)

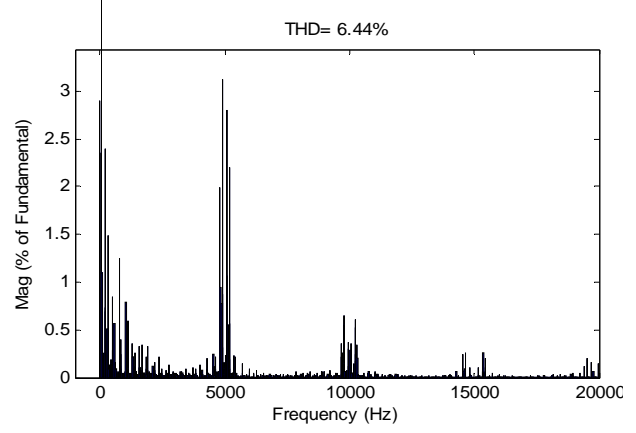


(b)

Fig. 10 Steady state current along with THD with HPWM algorithm for $M_i = 0.81$



(a)



(b)

Fig. 11 Steady state current along with THD with SVPWM algorithm for $M_i = 0.9$

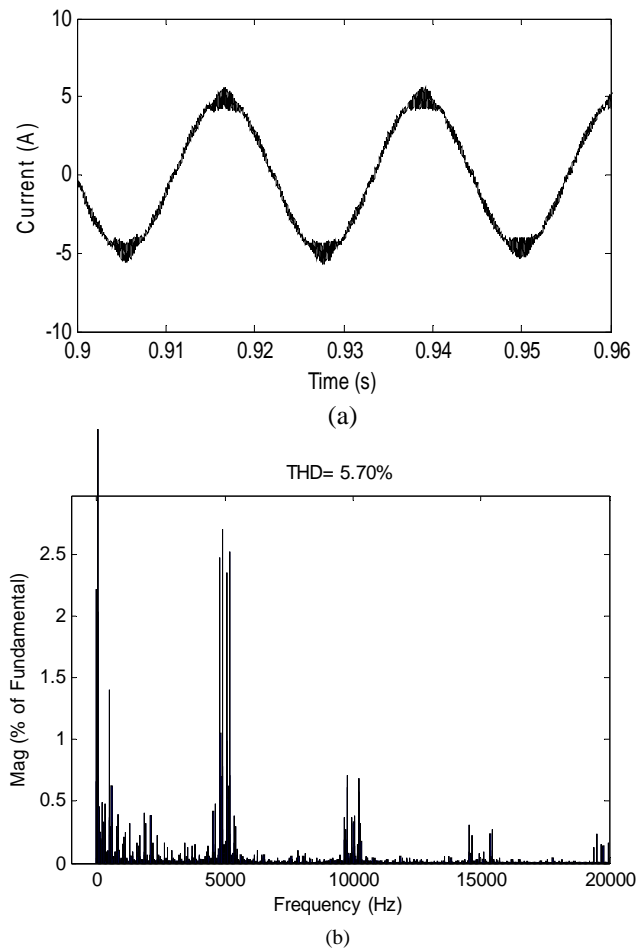


Fig. 12 Steady state current along with THD with HPWM algorithm for $M_i = 0.9$

To develop the proposed algorithm, here harmonic flux ripple characteristics are plotted for each PWM sequence and a sequence that gives less harmonic distortion is used at every sampling interval. The simulation results show the effectiveness of the proposed algorithm.

REFERENCES

- [1] [1] Joachim Holtz, "Pulsewidth modulation – A survey", *IEEE Trans. Ind. Electron.*, Vol. 39, No.5, pp. 410-420, Dec. 1992..
- [2] G. Narayanan and V. T. Ranganathan, "Triangle comparison and space vector approaches to pulse width modulation in inverter-fed drives," *J.Indian Inst. Sci.*, vol. 80, pp. 409–427, Sep/Oct, 2000.
- [3] Heinz Willi Van Der Broeck, Hans-Christoph Skudelny and Georg Viktor Stanke, "Analysis and realization of a pulsewidth modulator based on voltage space vectors", *IEEE Trans. Ind. Applic.*, Vol. 24, No.1, pp.142-150, Jan/Feb 1998.
- [4] H. Krishnamurthy, G. Narayanan, V.T.Ranganathan, R. Ayyar, "Design of space vector-based hybrid PWM techniques for reduced current ripple" *IEEE-APEC*, Vol.1, pp 583-588, 2003.
- [5] G.Narayanan, Di Zhao, H. Krishnamurthy and Rajapandian Ayyanar, "Space vector based hybrid techniques for reduced current ripple" *IEEE Trans. Ind. Applic.*, Vol. 55, No.4, pp.1614-1626, April 2008.
- [6] Vladimir Blasko, "Analysis of a hybrid PWM based on modified space-vector and triangle-comparison methods" *IEEE Trans. Ind. Applicat.*, vol. 33, no. 3, May/June 1997, pp. 756-764.
- [7] T. Brahmananda Reddy, J. Amarnath and D. Subbarayudu, "Improvement of DTC performance by using hybrid space vector pulsewidth modulation algorithm" *International Review of Electrical Engineering*, Vol.4, no.2, pp. 593-600, Jul-Aug, 2007.
- [8] Ahmet M. Hava, Russel J. Kerkman and Thomas A. Lipo, "Simple analytical and graphical methods for carrier-based PWM-VSI drives" *IEEE Trans. Power Electron.*, vol. 14, no. 1, Jan 1999, pp. 49-61
- [9] Joohn-Sheok Kim and Seung-Ki Sul, "A novel voltage modulation technique of the space vector PWM", in *Conf. Rec. IPEC'95*, Yokohama, Japan, 1995, pp. 742-747.
- [10] Dae-Woong Chung, Joohn-Sheok Kim, Seung-Ki Sul, "Unified voltage modulation technique for Real-Time three-phase power conversion" *IEEE Trans. On Ind. Applications*, vol. 34, no.2, pp 374-380, March/April, 1998.
- [11] I. S. Jacobs and C. P. Bean, "Fine particles, thin films and exchange anisotropy," in *Magnetism*, vol. III, G. T. Rado and H. Suhl, Eds. New York: Academic, 1963, pp. 271–350.
- [12] K. Elissa, "Title of paper if known," unpublished.
- [13] R. Nicole, "Title of paper with only first word capitalized", *J. Name Stand. Abbrev.*, in press.
- [14] Y. Yoroazu, M. Hirano, K. Oka, and Y. Tagawa, "Electron spectroscopy studies on magneto-optical media and plastic substrate interface," *IEEE Transl. J. Magn. Japan*, vol. 2, pp. 740–741, August 1987 [Digests 9th Annual Conf. Magnetics Japan, p. 301, 1982].
- [15] M. Young, *The Technical Writer's Handbook*. Mill Valley, CA: University Science, 1989.